Application of Multiresolution Analyses to Electron Density Maps: A Critical Point Analysis Approach for the Comparison of Molecules

L. LEHERTE, N. MEURICE, D. P. VERCAUTEREN
Laboratoire de Physico-Chimie Informatique
Facultés Universitaires Notre-Dame de la Paix
Rue de Bruxelles 61, B-5000 Namur
BELGIUM

Abstract: - A procedure is proposed for the comparison of molecules. It is based on graph representations of electron density maps smoothed using three different methods: simulation of an X-ray diffraction experiment, wavelet-based multiresolution analysis, and analytical smoothing. Graph representations are obtained using a critical point analysis method. Multiple comparisons between the critical point graphs are then carried out using a simulated annealing technique. Results are compared with literature data.

Key-Words: - Multiresolution Analysis, Wavelets, Electron Density, Critical Points, Molecular Similarity

1 Introduction

Even with the advance of supercomputers, most of the properties of very large systems, like biomolecules, can be accessed only with simplified models. For example, in proteins, amino acid residues can be depicted using a lower level representation, *i.e.*, two or three pseudo-atoms rather than by an all-atom representation. Simplified representations of protein geometry were also used to reduce sensitivity to small perturbations in conformation, *e.g.*, when docking a ligand *vs.* a receptor. Cherfils *et al.* [1] replaced amino acid residues with spheres of varying size and performed docking to maximize the buried surface area. Simulating proteins at low resolution is also a way to overcome structural inaccuracies [2] issued from NMR data or from an approximate modeling. Vakser *et al.* [2] digitized a protein image onto a three-dimensional (3D) grid. The structural elements smaller than the grid step were thus eliminated from the structure. In molecular graphics, fast comparison of protein structures at a predetermined level of detail was suggested through the use of B-spline functions and wavelet analysis [3] while Ritchie *et al.* [4] proposed a different mathematical representation of protein molecular shapes in terms of low resolution real spherical harmonics.

The grouping of atoms together was also achieved to model small molecules. For example, Takahashi *et al.* [5] described organic structures in terms of graphs wherein each node represents a functional group and the edge between any two nodes is weighted by the topological path length (the number of bonds).

Low resolution representations are also extremely useful in the refinement or interpretation of images generated by experimental approaches such as electron microscopy or X-ray diffraction. For example, high resolution structures of individual elements of a macromolecular complex are created and imaged at lower resolution to validate the interpretation of a low resolution image of the complex [6].

The principle of multiresolution analysis (MRA) based on wavelet theory is shown to be a procedure useful in discovering low resolution information hidden behind high resolution features. It is also adapted to the restoration of noisy images [7]. Performing a MRA consists in the decomposition of an image into its details corresponding to a range of resolution levels. A particular application in the field of chemistry can be found in [8] wherein MRA was applied to restore 2D X-ray topographs damaged by Gaussian noise.

The aim of the work presented in this paper consists in assessing low resolution representations of electron density (ED) distributions in their ability to determine similarity between various molecular structures.

Comparing several molecules, all with a common property, *e.g.*, biological affinity, can help to understand the binding mode between a receptor and a guest molecule when the structure of the host molecule is not available. A similarity quantifier applicable to steric and electrostatic

fields was for example developed by Carbo *et al.* [9]. However, orientation independent descriptors based on topology possess the obvious advantage of avoiding molecular translation and reorientation operations when matching two or more molecular structure properties.

2 Critical Point Analysis

A topological analysis method of 3D ED functions was established by Bader [10]. The topological properties of ED distributions can be described in terms of the number and kind of their critical points (CPs), *i.e.*, points where the gradient of the density is equal to zero. Each CP can be identified by its 3x3 Hessian matrix H(**r**) which is built on the local second derivatives of the ED function. The CPs are linked through a gradient vector field analysis to generate a graph whose vertices and edges are CPs and gradient trajectories, respectively. Popelier [11] has later extended this approach to include the concept of molecular similarity. The author proposes to use the properties of bond CPs (BCP), *i.e.*, density value, Laplacian, and ellipticity, extracted from *ab initio* wavefunctions. Similarly to Bader's approach, Johnson [12] developed a CP analysis method, based on Morse theory, for the location, identification, and connection of CP trees in experimental protein maps. His method, implemented in the program ORCRIT, was aimed at the automated interpretation of X-ray diffraction data for protein structures.

In the present work, the location of a CP in an ED distribution $\rho(\mathbf{r})$ is derived from Johnson's program [12] using the first derivative of ρ. The second derivatives are used to determine the nature of the CP by constructing the Hessian matrix:

$$H(\mathbf{r}) = \begin{pmatrix} \partial^2\rho/\partial x^2 & \partial^2\rho/\partial x\partial y & \partial^2\rho/\partial x\partial z \\ \partial^2\rho/\partial y\partial x & \partial^2\rho/\partial y^2 & \partial^2\rho/\partial y\partial z \\ \partial^2\rho/\partial z\partial x & \partial^2\rho/\partial z\partial y & \partial^2\rho/\partial z^2 \end{pmatrix} \quad (1)$$

This matrix is then diagonalized and the three non-zero diagonal elements, the eigenvalues, are used to determine the type of CP of the ED map. When the number of negative eigenvalues, n_E, is equal to 3, the CP corresponds to a local maximum or peak. A point where n_E=2 is a saddle point or pass. n_E=1 corresponds to a saddle point or pale, while n_E=0 characterizes a pit.

3 Multiresolution Analysis

In order to reduce the number of data points, it is essential to translate the pixel representation of a 3D property into a simpler one that still captures the relevant shape information and discard the unnecessary details. To our knowledge, only few applications of MRA to chemical sciences, particularily to structural chemistry, exist. In practice, wavelet theory is most commonly applied to the treatment of signal processing in analytical chemistry and for the representation of wavefunctions and orbitals in electronic structure calculations [13]. In order to modify the resolution of an ED map, three procedures were elaborated which are described hereafter.

3.1 Crystallographic Resolution

In crystallography, the resolution of an ED map is defined by the ratio $\sin\Theta/\lambda$, where 2Θ is the angle between the diffracted X-ray and the primary beam of wavelength λ. The ED $\rho(\mathbf{r})$ is calculated as the Fourier transform of an adequate set of structure factors $F(\mathbf{h})$ computed in the reciprocal space according to the input molecular structure $\{\mathbf{r}_i\}$, the resolution, and the tabulated atom scattering factors $\{f_i\}$:

$$\rho(r) = \hat{F}(h) \text{ with } F(h) = \sum_{i=1}^{nat} f_i \, e^{\left(\frac{\sin\Theta}{\lambda}\right)^2} \, e^{-2\pi i \, r_i . h} \quad (2)$$

The program XTAL [14] was used in the present work to generate ED maps at a selected 3 Å medium resolution [15] from crystalline parameters and atom positions. Two other approaches, based on Quantum Mechanical calculations, and which do not require the knowledge of any crystal parameters were also considered. Both methods, implemented in in-house programs [16, 17], are presented below.

3.2 Atomic Shell Approximation (ASA)

A promolecular ED distribution ρ_M is calculated as a weighted summation over atomic ED distributions ρ_a which are described in terms of five-terms series of 1s Gaussian functions fitted from atomic 3-21G basis set representations [18]:

$$\rho_M = \sum_a Z_a \, \rho_a \quad (3)$$

where Z_a is the atomic number of atom a, and:

$$\rho_a(\mathbf{r} - \mathbf{R}_a) = \sum_{i=1}^{5} w_{a,i} \left(\left(\frac{2\zeta_{a,i}}{\pi} \right)^{3/4} e^{\zeta_{a,i} |\mathbf{r} - \mathbf{R}_a|^2} \right)^2 \quad (4)$$

$\mathbf{R}_a$ being the position vector of atom a, and $w_{a,i}$ and $\zeta_{a,i}$, the fitted parameters, respectively.

A smoothed version of such a molecular ED representation is computed using the formalism presented by Kostrowicki *et al.* [19]:

$$\rho_{a,t}(\mathbf{r}-\mathbf{R}_a) = \sum_{i=1}^{5} a_{a,i}\left(1+8b_{a,i}t\right)^{-3/2} e^{\frac{-b_{a,i}|\mathbf{r}-\mathbf{R}_a|^2}{1+8b_{a,i}t}} \quad (5)$$

wherein:

$b_{a,i} = 2\zeta_{a,i}$, $a_{a,i} = w_{a,i}\left(\frac{b_{a,i}}{\pi}\right)^{6/4}$, and t is the smoothing parameter.

3.3 Wavelet Transforms

A wavelet transform (WT) is a localized transform in both space (time) and frequency which uses integration kernels called wavelets [20]. A basis set of wavelet functions $\Psi_{ab}(x)$ is built on translated and dilated versions of a so-called mother wavelet $\Psi(x)$:

$$\Psi_{ab}(x) = \frac{1}{\sqrt{|a|}}\,\Psi\left(\frac{x-b}{a}\right) \text{ with } a \in R_0,\ b \in R \quad (6)$$

where a is the scaling parameter which allows to capture changes in frequency, and b is the shift along the x axis applied in order to analyze space-dependent variations of a signal. The projection of a square integrable signal f onto this basis according:

$$Wf(a,b) = \int_{-\infty}^{+\infty} f(x)\,\Psi^{*}_{ab}(x)\,dx = \langle f, \Psi_{ab}\rangle \quad (7)$$

is the result from the WT. The continuous WT can be discretized by restricting a and b to the points of a dyadic lattice ($a = 2^{-j}$, $b/a = 1$). In this context, the construction of the so-called Daubechies wavelet functions [21] is derived from a MRA which is a mathematical construction used to express an arbitrary function f at various levels of detail. f(x) is developed as a series of wavelets $\Psi_{jk}(x)$:

$$f(x) = \sum_j \sum_k d_{jk}\,\Psi_{jk}(x) \quad (8)$$

$d_{jk} = \langle f, \Psi_{jk}\rangle$ being called the wavelet coefficients.

A Fast WT (FWT) is performed by a set of low- and high-pass filters, the scaling function Φ, and the wavelet function Ψ, respectively. In practice, the wavelet expansion is truncated at some scale J:

$$f(x) = \sum_k c_{Jk}\,\Phi_{Jk}(x) + \sum_{j=J}^{J_0-1} \sum_k d_{jk}\,\Psi_{jk}(x) \quad (9)$$

where J_0 is the resolution of the original signal. In the decomposition, the function is convolved with Φ and Ψ. Each resulting function is decimated by suppression of one data out of two. In the case of a multi-dimensional signal, the FWT algorithm can easily be applied to each dimension separately. Many detail images are thus obtained. The reconstruction of a smoothed version of a signal can be done by cancelling all detail coefficients and processing the inverse WT of the signal.

A WT for discrete data, known as the *à trous* algorithm [7], is a redundant transform wherein decimation is not carried out. This approach was selected in the present work since it presents two advantages: symmetrical filters can be used and only one detail image is obtained at each level of resolution: $d_{j-1,k} = c_{jk} - c_{j-1,k}$.

4 Molecular Comparisons

Benzodiazepine-related compounds (BZ) belong to an important family of molecules with various pharmacological effects. The understanding of the interaction mechanisms between the guest molecules and their receptor whose 3D structure is still unsolved is unclear. The determination of a pharmacophore model (a set of functional groups and their geometrical arrangement necessary to explain a given binding property) is thus a major concern for scientists in this field of research.

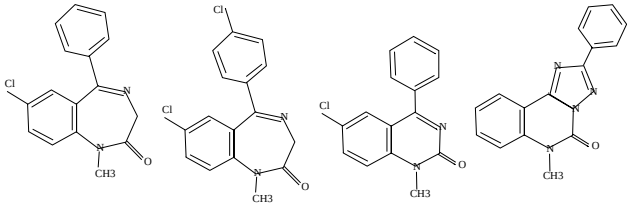

Diazepam Ro5-4864 QUIZ TZQ

Fig. 1 Planar structure formulas of benzodiazepine-related compounds.

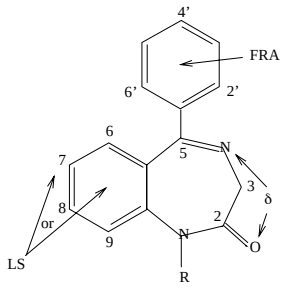

Fig. 2 Schematic representation of the most frequently described pharmacophore features common to BZ ligands.

A limited number of ligands was selected (Fig. 1): *Diazepam* (7-chloro-1, 3-dihydro-1-methyl-5-(phenyl)-2H-1, 4-benzodiazepin-2-one), *Ro5-4864* (7-chloro-1, 3-dihydro-1-methyl-5-(p-chlorophenyl)-2H-1, 4-benzodiazepin-2-one), *QUIZ* (6-chloro-N1-methyl-4-phenylquinazolin-2-one), and *TZQ* ([1, 2, 4]triazolo[1, 5-c]quinazolin-5(6H)-one). Several pharmacophore models have already been published [22]. They all present common elements (Fig. 2): a freely rotating

aromatic group (FRA), a lipophilic and/or steric group (LS), and one or two H-attractor groups (δ).

4.1 Electron Density Map Calculations

The 3D atomic coordinates of the considered ligands were derived from crystallographic data. Two structures are reported in the Cambridge Crystallographic Database [23]: Diazepam (DIZPAM10) and Ro5-4864 (FULWUE). Atomic coordinates of molecules TZQ and QUIZ were obtained from X-ray diffraction experiments in our institution. Within the crystallographic approach, 64x32x64 (16x8x16 Å) ED maps were generated using XTAL [14] at a resolution of 3 Å, using the P_1 space group operations. This guarantees that packing effects, which do not occur under biological conditions, do not affect the CP representation of individual molecules. Atomic Shell Approximation (ASA) ED functions were generated analytically with a smoothing parameter equal to 0.790, and *ab initio* 6-31G** RHF MO-LCAO-SCF calculations were carried out in order to obtain 128x64x128 full ED maps with a grid interval of 0.125 Å. For the WT approach, the filter Φ that was selected to smooth the original *ab initio* images is the convolution product of the Daubechies' filter of order 2 [24]: $\Phi = (-\sqrt{2}/32,\ 0,\ 9\sqrt{2}/32,\ \sqrt{2}/2,\ 9\sqrt{2}/32,\ 0,\ -\sqrt{2}/32)$.

4.2 Critical Point Analysis Results

Graph representations of medium resolution ED maps obtained through simulations of X-ray diffraction experiments at 3 Å (XTAL), using the WT smoothing, and analytical smoothing (ASA), are presented in Figs. 3, 4, and 5, respectively, wherein peaks and passes are numbered according to their decreasing ρ value (Table 1). In order to get graphs that are similar to those generated in Fig. 3, the WT smoothing must be applied up to the fourth level of resolution (J = 4), and the ASA smoothing has to be carried out with t = 0.790. At such resolution levels, structurally different molecules, such as TZQ with respect to the other BZ-related compounds, adopt a similar representation. Graph topologies are either a 3-branches star, or a bended unbranched segment with peaks that are located on chlorine atoms (when present), free phenyl groups, and N or C=O groups. Very interestingly, these peaks correspond to the pharmacophore elements described in Fig. 2.

Table 1. Density values ρ ($e^-/Å^3$) of the peaks generated by the program ORCRIT applied to smoothed ED maps using XTAL (ρ), WT smoothing (ρx100), and ASA smoothing (ρx10) for Diazepam (D), Ro5-4864 (R), QUIZ (Q), and TZQ (T).

		LS	FRA	N	C=0
XTAL	D	2.81	1.78	1.97	2.07
	R	2.78	2.41	2.00	1.94
	Q	2.86	1.79	-	2.43
	T	2.20	2.01	2.42	2.33
WT	D	4.05	3.11	2.79	3.20
	R	4.11	3.89	-	3.19
	Q	4.11	2.92	-	3.35
	T	3.05	2.99	3.70	3.30
ASA	D	1.80	1.30	1.37	1.48
	R	1.81	1.80	1.37	1.47
	Q	1.81	1.31	-	1.47
	T	1.27	1.29	1.65	1.54

Examination of Table 1 and Figs. 3-5 shows that, very logically, Cl atoms lead to higher density peaks than the other groups. The ASA smoothing approach tends to level out density values, and CPs within fused rings are not detected by the numerical approach implemented in ORCRIT. This last approach thus leads to less discriminating graphs.

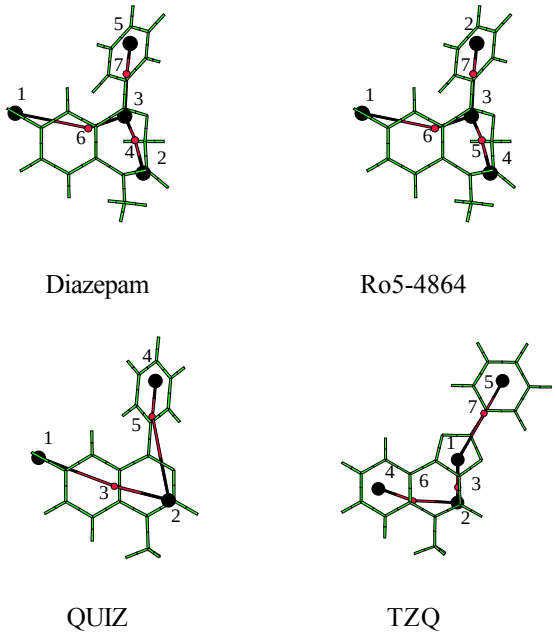

Fig. 3. Graphs of CPs (large spheres = peaks, small spheres = passes) of promolecular 3 Å resolution ED maps generated using XTAL.

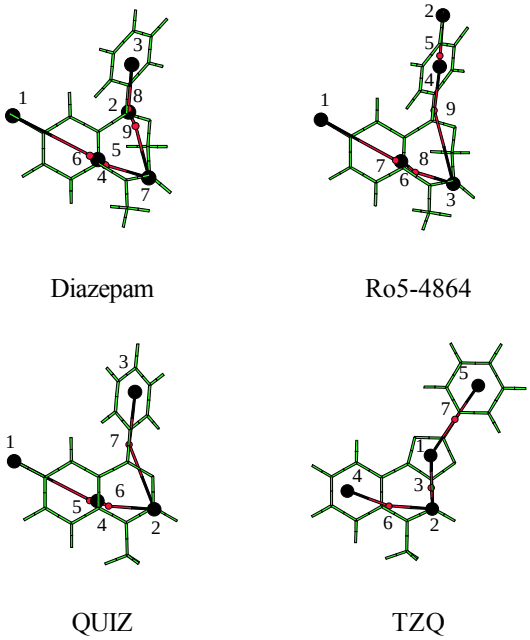

Fig. 4. Graphs of CPs (large spheres = peaks, small spheres = passes) of *ab initio* full ED maps generated using the WT smoothing.

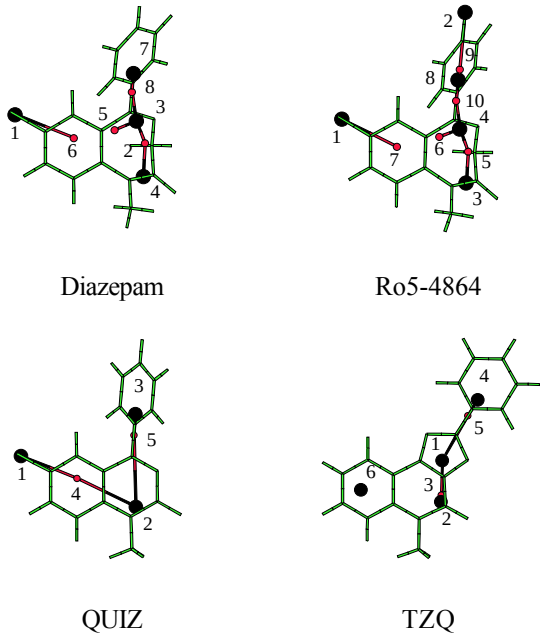

Fig. 5. Graphs of CPs (large spheres = peaks, small spheres = passes) of promolecular ED maps generated using the ASA smoothing.

The crystallographic approach is very fast (~30") on an IBMR6K model 580, but presents the disadvantage of generating unwanted background CPs resulting from the FFT error truncation that is implemented in XTAL. It is also limited to promolecular descriptions of molecular ED distributions. The WT procedure is reasonably fast (~100"), but follows the lengthy calculation of *ab initio* ED maps (~45'). The resolution levels that can be modeled are also strongly dependent on the grid interval of the ED maps. But the great advantage of the WT method is that it can be applied to any n-D molecular property. The analytical ASA approach requires intermediate computing times (~210" for a 64x32x64 grid), and the resolution, which is determined by the value of t, can be varied continuously. However, it requires an analytical expression of the molecular property that is considered.

4.3 Multiple Superposition Results

A simulated annealing (SA) algorithm [25] was used to match each set of four CP graphs, each graph being represented as a 2D array (diagonal elements = density values (ρ_{peak}+10, ρ_{pass}), off-diagonal elements = distances between vertices). The simulation consisted in a sequence of Monte Carlo (MC) sampling procedures that were carried out at progressively decreasing rates of acceptance:

$$p = \exp(-\beta\ \mathrm{rms}) \qquad (10)$$

with an evaluation function:

$$\mathrm{rms} = \sqrt{\frac{1}{n_x n_p}\sum_{i=1}^{n_x n_p}\left(\rho_i - \rho_i^{ref}\right)^2 + \frac{1}{m_x n_p}\sum_{i=1}^{m_x n_p}\left(d_i - d_i^{ref}\right)^2} \qquad (11)$$

where m is the number of distances between the n points of a completely connected graph, and n_p, the total number of pairs of graphs that can be built from the molecules to be compared. In this formula, the ρ- and d-dependent terms have a similar weight. A lower weight for the d-term might be considered in order to take into account molecular flexibility, for example.

Each SA run consisted in 21 MC procedures (each of 200000 iterations) that were carried out with β ranging between 0.05 and 1, and took about 4' on a IBMR6K model 580. Two different superposition strategies were used: (a) the number of points to be matched in each graph is equal to the total number of points *n* in the smallest graph, or is equal to *n-1*, in order to avoid matching between physically unrelated CPs. Critical point matching results were then translated into visual molecular superimpositions using the program QUATFIT [26]. Quaternary superposition results, corresponding to the lowest rms values obtained within each strategy are presented in Table 2 and Fig. 6 wherein TZQ is shown in black. In each case, the solution observed with the lowest rms value is a standard one, *i.e.*, it corresponds to the matching of the CP graphs according to the known

pharmacophore description. In the second solution, TZQ is inverted, *i.e.*, its FRA CP is matched with the LS CP of the other compounds. This is consistent with a renaming of the FRA element into a LS element by the scientific community [22].

Table 2. Superposition results obtained using a SA algorithm for the comparison of the CP graphs of Diazepam, QUIZ, TZQ, and Ro5-4864 (D, Q, T, R).

XTAL	n	D	1	4	2	5	7		
		Q	1	3	2	4	5		
		T	4	3	2	5	7		
		R	1	6	3	2	7		
	n-1	D	5	6	7	1			
		Q	4	3	5	1			
		T	2	7	3	5			
		R	3	7	6	2			
WT	n	D	8	2	6	1	3	4	5
		Q	7	2	5	1	3	4	6
		T	7	1	6	4	5	2	3
		R	9	3	7	1	4	6	8
	n-1	D	6	4	5	3	2	8	
		Q	5	4	6	3	2	7	
		T	6	2	3	5	1	7	
		R	7	6	8	4	3	9	
ASA	n	D	7	3	6	1	8		
		Q	3	2	4	1	5		
		T	4	1	3	6	5		
		R	8	4	7	1	10		
	n-1	D	1	7	8	6			
		Q	1	3	5	4			
		T	4	2	3	5			
		R	1	8	10	7			

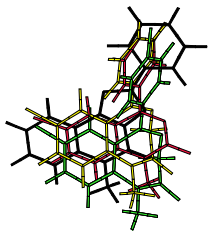

XTAL n-points
rms = 1.09

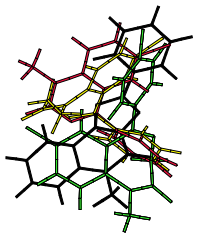

XTAL (n-1)-points
rms = 0.89

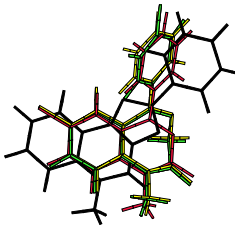

WT n-points
rms = 1.05

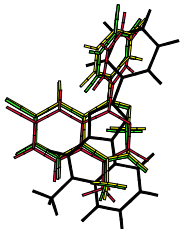

WT (n-1)-points
rms = 0.98

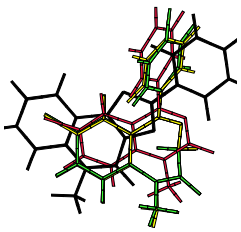

ASA n-points
rms = 0.87

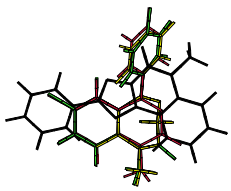

ASA (n-1)-points
rms = 0.67

Fig. 6. n- and (n-1)-points molecular superimpositions of SA solutions resulting from the alignment of BZ graphs obtained using a CP analysis of ED distributions obtained with XTAL, the WT smoothing, and the ASA approach.

5 Conclusion

A simulated annealing procedure was applied to critical point (CP) graphs representations of smoothed electron density distribution functions of small pharmacological ligands. Three different smoothing approaches were developed and implemented which led to very similar results. The crystallographic method is the fastest, but the wavelet-based multiresolution analysis is applicable to any grid representation of a molecular property. The analytical approach presents the advantage to be continuously scalable, but requires an analytical description of the molecular property. An analytical search for CP using a symbolic language is now under investigation. The obtained low resolution CP graphs revealed the pharmacophore structure of the ligands, and generalization of the CP analysis results to other molecules is now under progress. It is suggested that the binding of a molecule *vs.* a receptor can be described at various levels of resolution, from the lowest which contain information about the global shape of a molecule, to the highest at which detailed H-bond, and van der Waals are described, *via* intermediate ones which reveal functional groups.

Acknowledgments

LL wishes to thank C.K. Johnson for providing the program ORCRIT. She also thanks S. Fortier, J.I. Glasgow, F.H. Allen, and H. Chermette for fruitful discussions. All the authors thank J.-P. Antoine for a discussion about non-orthogonal wavelets, L. Piela for discussing analytical smoothing, and the FUNDP for the use of the Namur Scientific Computing Facility (SCF) Center.

References:

[1] J. Cherfils, S. Duquerroy and J. Janin, Protein-Protein Recognition Analyzed by Docking Simulation, *Protein*, Vol. 11, 1991, pp. 271-280.

[2] I.A. Vakser, O.G. Matar and C.F. Lam, A Systematic Study of Low-Resolution Recognition in Protein-Protein Complexes, *Proc. Natl. Acad. Sci. USA*, Vol. 96, 1999, pp. 8477-8482.

[3] M. Carson, Wavelets and Molecular Structure, *J. Comp.-Aided Mol. Des.*, Vol. 10, 1996, pp. 273-283.

[4] D.W. Ritchie and G.J.L. Kemp, Fast Computation, Rotation, and Comparison of Low Resolution Spherical Harmonic Molecular Surfaces, *J. Comput. Chem.*, Vol. 20, 1999, pp. 383-395.

[5] Y. Takahashi, M. Sukekawa and S.-I. Sasaki, Automatic Identification of Molecular Similarity Using Reduced-Graph Representation of Chemical Structure, *J. Chem. Inf. Comput. Sci.*, Vol. 32, 1992, pp. 639-643.

[6] T.S. Baker and J.E. Johnson, Low Resolution Meets High: Towards a Resolution Continuum from Cells to Atoms, *Curr. Opin. Struct. Biol.*, Vol. 6, 1996, pp. 585-594.

[7] J.-L. Stark, F. Murtagh and A. Bijaoui, *Image Processing and Data Analysis - The Multiscale Approach*, Cambridge University Press, Cambridge, UK, 1997.

[8] M. Pilard and Y. Epelboin, Multiresolution Analysis for the Restoration of Noisy X-ray Topographs, *J. Appl. Cryst.*, Vol. 31, 1998, pp. 36-46.

[9] R. Carbo, B. Calabuig, L. Vera and E. Besalu, Molecular Quantum Similarity: Theoretical Framework, Ordering Principles, and Visualization Techniques, *Adv. Quantum Chem.*, Vol. 25, 1994, pp. 253-313.

[10] R.W. Bader, *Atoms in Molecules - A Quantum Theory*, Clarendon Press, Oxford, 1995.

[11] P.L.A. Popelier, Quantum Molecular Similarity. 1. BCP Space, J. Phys. Chem. A, Vol. 103, 1999, pp. 2883-2890.

[12] C.K. Johnson, *ORCRIT. The Oak Ridge Critical Point Network Program*, Technical report. Chemistry Division, Oak Ridge National Laboratory, Oak Ridge, TN, 1977.

[13] A.K.-M. Leung, F.-T. Chau and J.-B. Gao, A Review on Applications of Wavelet Transform Techniques in Chemical Analysis: 1989-1997, Chemometrics and Intelligent Laboratory Systems, Vol. 43, 1998, pp. 165-184, and references therein.

[14] *XTAL 3.0 User's Manual*, eds. S.R. Hall and J.M. Stewart, Universities of Western Australia and Maryland, 1990.

[15] L. Leherte, N. Meurice and D.P. Vercauteren, Critical Point Representation of Electron Density Maps for the Comparison of Benzodiazepine-type Ligands, *J. Chem. Inf. Comput. Sci.*, in press.

[16] L. Leherte, *ATROUS*, FUNDP, Namur, Belgium, 1998.

[17] L. Leherte, *ASA_SMOOTH*, FUNDP, Namur, Belgium, 2000.

[18] L. Amat and R. Carbo-Dorca, Quantum Similarity Measures under Atomic Shell Approximation: First Order Density Fitting Using Elementary Jacobi Rotations, *J. Comput. Chem.*, Vol. 19, 1997, pp. 2023-2039.

[19] J. Kostrowicki, L. Piela, B.J. Cherayil and H.A. Scheraga, Performance of the Diffusion Equation Method in Searches for Optimum Structures of Clusters of Lennard-Jones Atoms, *J. Phys. Chem.*, Vol. 95, 1991, pp. 4113-4119.

[20] G. Strang and T. Nguyen, *Wavelets and Filter Banks*, Wellesley-Cambridge Press, Wellesley, MA, USA, 1997.

[21] I. Daubechies, Orthonormal Bases of Compactly Supported Wavelets, *Commun. Pure Appl. Math.*, Vol. 41, 1988, pp. 909-996.

[22] J.-J. Bourguignon, Endogeneous and Synthetic Ligands of Mitochondrial Benzodiazepine Receptors: Structure-Affinity Relationships, in: *Peripheral Benzodiazepine Receptors*, ed. E. Giesen-Crouse, Academic Press, San Diego (CA), 1993, pp. 59-85; and personnal communication.

[23] F.H. Allen, J.E. Davies, J.J. Galloy, O. Johnson, O. Kennard, C.F. Macroe, E.M. Mitchell, G.F. Smith, D.G. Watson, The Development of Versions 3 and 4 of the Cambridge Structural Database System, *J. Chem. Inf. Comput. Sci.*, Vol. 31, 1991, pp. 187-209.

[24] M.J. Shensa, The Discrete Wavelet Transform: Wedding the A Trous and Mallat Algorithms, *IEEE Trans. Signal Processing*, Vol. 40, 1992, pp. 2464-2482.

[25] L. Leherte, *GRAPH_SUP*, FUNDP, Namur, Belgium, 1998.

[26] D.J. Heisterberg, Ohio Supercomputer Center, Colombus, OH. Translation from Fortran to C and input/output by J. Labanowski, Ohio Supercomputer Center, Columbus, OH, 1990.